

Time series analysis of ionization waves in dc neon glow discharge

M. A. Hassouba, H. I. Al-Naggar, and N. M. Al-Naggar
Department of Physics, Faculty of Science, Benha University, Egypt

C. Wilke
Institute of Physics, E. M. A. University, Domstrasse 10a, 17489 Greifswald, Germany

(Received 28 March 2006; accepted 6 June 2006)

The dynamics of dc neon glow discharge is examined by calculating a Lyapunov exponent spectrum (LES) and correlation dimension (D_{corr}) from experimental time series. The embedding theory is used to reconstruct an attractor with the delay coordinate method. The analysis refers to periodic, chaotic, and quasi-periodic attractors. The results obtained are confirmed by a comparison with other methods of time series analysis such as the Fourier power spectrum and autocorrelation function. The main object of the present work is the positive column of a dc neon glow discharge. The positive column is an excellent model for the study of a non-linearity plasma system because it is nonisothermal plasma far from equilibrium. © 2006 American Institute of Physics.
 [DOI: 10.1063/1.2219420]

I. INTRODUCTION

Plasma is a typical nonlinear dynamics system with a large number of degrees of freedom; it is of interest as a medium for testing the universal characteristics of chaos. In the past decade, a number of nonlinear dynamics phenomena have been studied in gas discharge plasmas.¹⁻⁷ Quasi-periodic transitions to chaos have been observed in plasmas.⁸ The understanding of quasi-periodic attractors and the related strange nonchaotic attractors is significant not only in nonlinear dynamics but also in plasmas. Analysis of time series from dynamical systems is an important issue in many different fields of engineering and science. The most common tools for this analysis are the Fourier power spectrum (FPS), correlation dimension (D_{corr}), and Lyapunov exponent spectrum (LES).

The aim of the present work is to study and investigate the state of the plasma of ionization waves of dc neon glow discharge in the region near the anode of the positive column region.

The experiment was performed in a sealed cylindrical discharge tube (Pyrex glass) filled with pure neon gas at a pressure of $p=3.4$ Torr. The tube had an internal radius of $r=2.0$ cm and the separation distance between the two electrodes (cold hollow cathode and plane anode) was fixed at $L=70$ cm. Discharge operation was sustained by an external voltage and the discharge current I limited by a load resistor $R=50$ k Ω (see Fig. 1). If the discharge current exceeds a low-current threshold, the positive column of the discharge destabilizes through the ionization instability. The discharge current I acts as a bifurcation parameter and variations of I allow one to observe coherent waves, quasi-periodic regimes, weak space-time chaos, and strange nonchaotic attractors. The light fluctuations are recorded near the anode with a sampling rate 500 kHz.

II. GEOMETRY OF PHASE-SPACE RECONSTRUCTION

In most cases only one characteristic quantity of experiment is obtained as a time series. Then a trajectory through m -dimensional phase space is reconstructed from this time series. According to the reconstruction theory: the reconstruction is valid for an embedding dimension (d_{embed}), $d_{\text{embed}} \geq 2d_{\text{attractor}} + 1$, and in the case of infinite data points $N \rightarrow \infty$, even for arbitrary delay times, where $d_{\text{attractor}}$ is the attractor dimension, this is a sufficient condition.^{9,10} There may be a lower embedding dimension. Therefore, procedures have to be found to allow both the choice of a suitable embedding dimension and a convenient delay time. It makes sense to choose d_{embed} as small as possible because it reduces the computing time for analysis of the reconstructed attractor such as correlation dimension and LES. On the other hand, the LES will not be falsified by the determination of false Lyapunov exponents, which appear if the embedding dimension is overestimated. So, the optimal value for d_{embed} is given by the false-nearest-neighbor method. At d_{embed} the attractor is unfold and this value is important in calculating LES and D_{corr} .

To calculate LES and D_{corr} , we reconstruct a dimension orbit d_m ,¹¹

$$\mathbf{x}_i = (x_i, x_{i+m}, x_{i+2m}, \dots, x_{i+(d-1)m}).$$

From the measured integrated light intensity $x(i\Delta t) \times (i=1 \dots N)$, with Δt being the sampling time interval, d_e is the embedding dimension, and $\tau=m\Delta t$ is the time delay. By choosing \mathbf{x}_j such that $|\mathbf{x}_j - \mathbf{x}_i| \leq r$ for small r , the evolution of small vectors $(\mathbf{x}_j - \mathbf{x}_i)$ can be obtained,

$$\mathbf{x}_{j+1} - \mathbf{x}_{i+1} = T_i(\mathbf{x}_j - \mathbf{x}_i).$$

We can decompose the matrix $T_i = Q_i R_i$ into orthogonal matrices Q_i and upper triangular matrices R_i . The Lyapunov exponent λ_i is given by

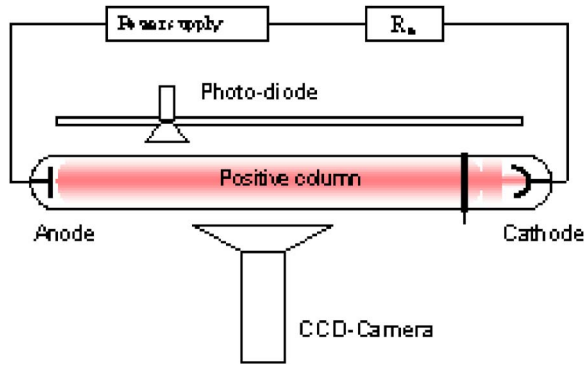


FIG. 1. Experimental setup; the light intensity is recorded with a photodiode.

$$\lambda_i = \frac{1}{K} \sum_{j=0}^{K-1} \ln(R_j)_{ii}, \quad i = 1, 2, \dots, d_m,$$

where K is a given number of matrices T_i . The Kaplan-Yorke dimension (D_{KY}) can be given from¹¹

$$D_{KY} = k + \frac{\sum_{i=1}^k \lambda_i}{|\lambda_{k+1}|},$$

where k is the maximum integer such that the sum of the k

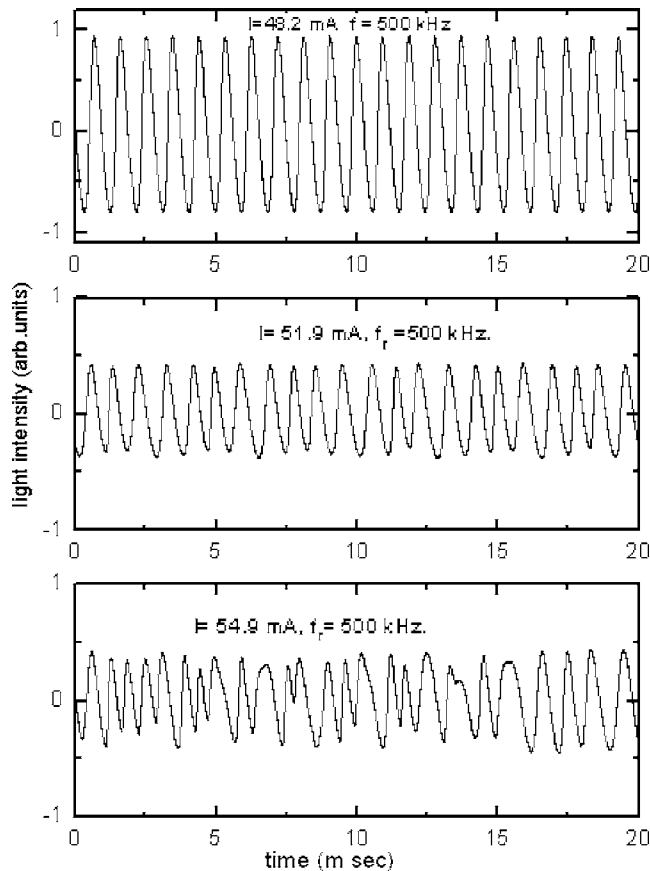


FIG. 2. Experimental time series for light intensity near the anode for dc neon glow discharge at different sampling currents: $I=48.2$, 51.9 , and 54.9 mA for sampling rate 500 kHz.

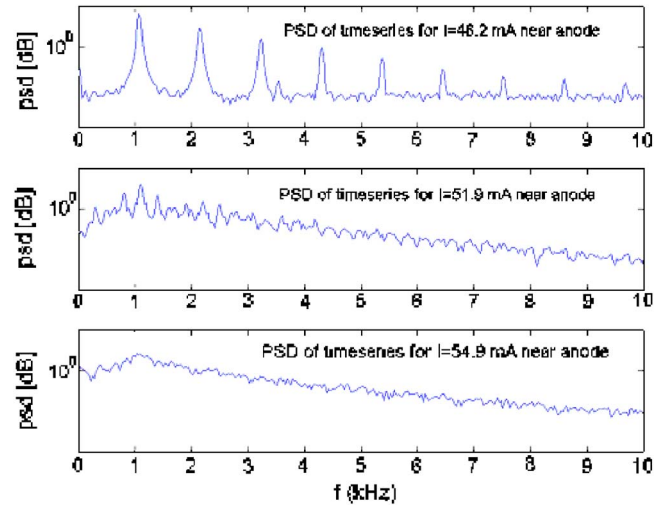


FIG. 3. Power spectrum density (PSD) for three different attractors at different currents: $I=48.2$, 51.9 , and 54.9 mA.

largest exponents is still non-negative. The Kaplan-Yorke dimension D_{KY} coincides with the correlation dimension.

We calculated the correlation dimension, which was introduced by Grassberger and Procaccia.^{12,13} First, one can define the correlation sum for a collection of points x_n in

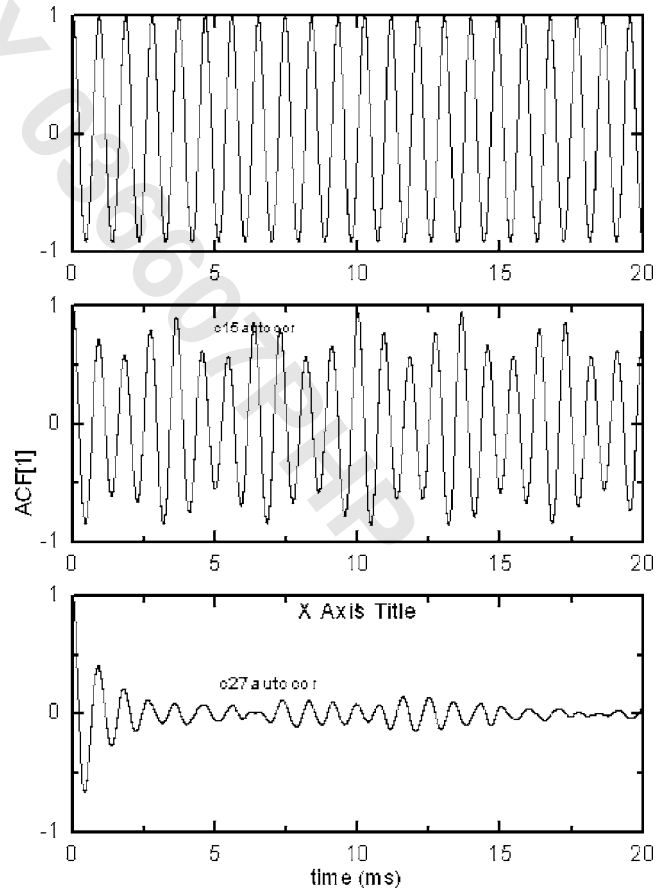


FIG. 4. Autocorrelation function (ACF) for three different experimental time series at three different discharge currents: $I=48.2$, 51.9 , and 54.9 mA.

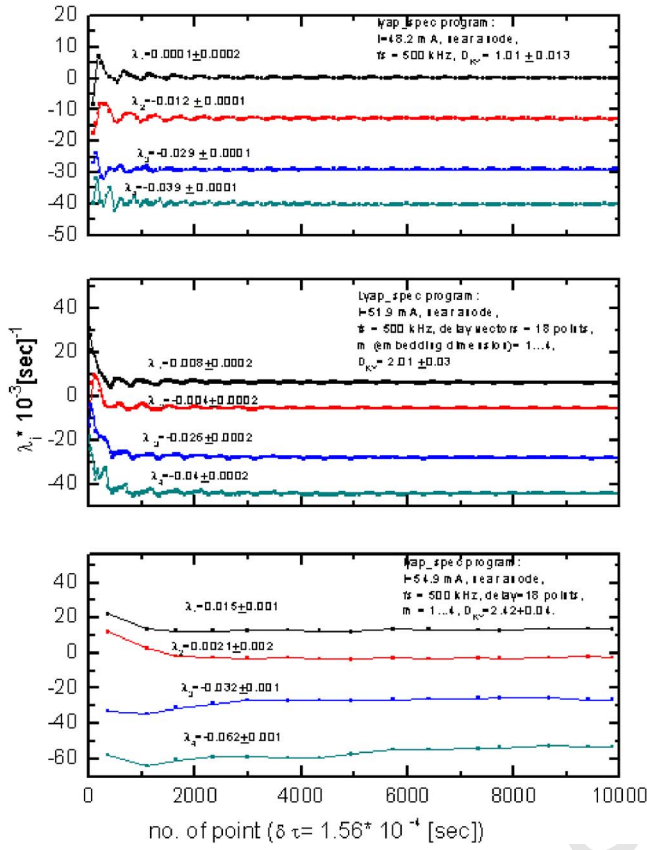


FIG. 5. Lyapunov exponent spectrum (LES) for three different experimental time series in Fig. 2 at three different currents: $I=48.2$, 51.9 , and 54.9 mA.

some vector space to be the fraction of all possible pairs of points, which are closer than a given distance r . Then the correlation dimension is defined as¹³

$$D_{\text{corr}} = \nu = \lim_{N \rightarrow \infty} \lim_{r \rightarrow 0} \frac{\log_2 C(m, r)}{\log_2 r},$$

where $C(m, r)$ is the correlation integral, which measures the number of points x_j that are correlated with each other in a sphere of radius ε around the reference points x_i ,¹²

$$C(m, r) = \frac{1}{N_{\text{ref}}} \frac{1}{N} \sum_{i=1}^{N_{\text{ref}}} \sum_{j=1}^N \vartheta(r - \|x_i - x_j\|),$$

where ϑ is the heavy side function ($\vartheta=0$ for the argument less than zero, otherwise $\vartheta=1$), N is the number of data points, and N_{ref} is the number of randomly chosen reference points (usually N_{ref} is smaller than N in order to save computation time). $\|x_i - x_j\|$ is the distance of two points along the curved manifold of the attractor. We usually measure the distance from the Euclidean norm as follows:¹⁴

$$\|x_i - x_j\| = \sqrt{\sum_{k=1}^d (x_{i,k} - x_{j,k})^2},$$

where d is the dimensionality of phase space. When $\log_2 C(r)$ is plotted versus $\log_2 r$ (log-log plot), then the slope of the resulting data may be a straight line or close to it.

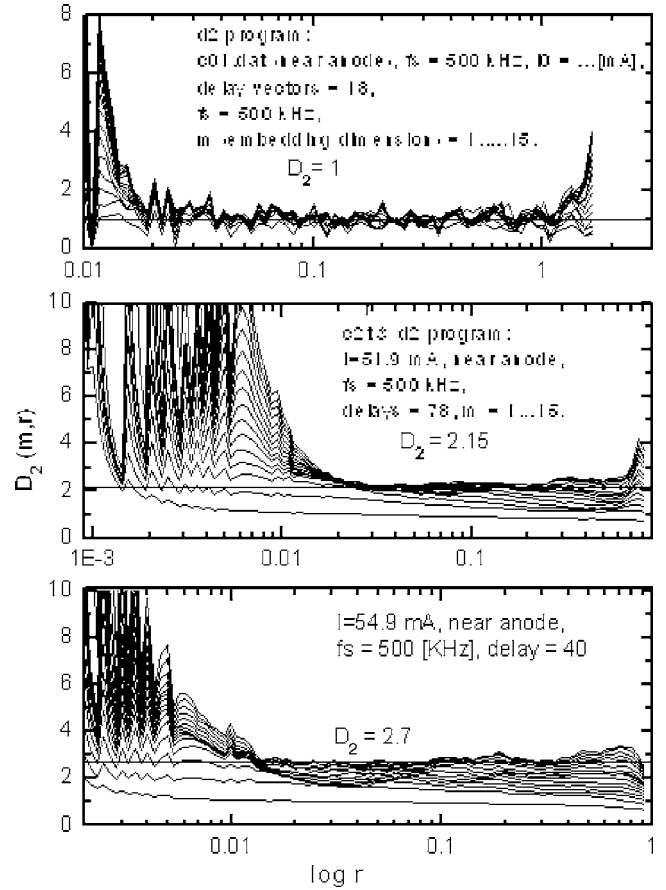


FIG. 6. Correlation dimension (D_{cor}) for three different experimental time series in Fig. 2 at three different currents: $I=48.2$, 51.9 , and 54.9 mA.

III. RESULTS AND DISCUSSION

The experimental time series for three different states of plasma are represented in Fig. 2, which analyzed at sampling rate 500 kHz at different sampling discharge current. These time series denote three different attractors.

The power spectrum density (PSD), which is calculated from the matlab program, is represented in Fig. 3. The PSD indicates whether the system is periodic or quasi-periodic. It is very good for the visualization of periodic and quasi-periodic phenomena and their separation from chaotic time evolutions. However, the analysis of the chaotic motions themselves does not benefit much from the PSD, because they lose phase information. This is essential for the understanding of what happens on a strange attractor. At $I=48.2$ mA, the PSD has multiple narrow peaks, which indicate a periodic attractor. At $I=51.9$ mA, the PSD shows the plasma state is a quasi-periodic attractor. At $I=54.9$ mA, the PSD is smooth continuous and the broad peak indicates that the attractor is a strange attractor. In order to confirm the type of the attractor, we calculated the correlation dimension and Lyapunov exponent spectrum.

The autocorrelation function (ACF) was derived from the time series data to classify the dynamic system: periodic, quasi-periodic, and chaotic attractor. The ACFs at different attractors are represented in Fig. 4. At $I=48.2$ mA, the ACF shows a periodic attractor; it is a sinusoidal wave and does

TABLE I. The results of numerical analysis for time series near the anode at the experimental parameters: $P=3.4$ Torr and $r=2$ cm.

Initial current (mA)	Sampling rate (kHz)	Correlation dimension	Lyapunov exponents (s^{-1})	Kaplan-York dimension (D_{KY})
$I=48.2$	500	1 (Periodic attractor)	$\lambda_1=0.0001\pm0.0002$ $\lambda_2=-0.012\pm0.0001$ $\lambda_3=-0.029\pm0.0001$	1.01 ± 0.013
$I=51.9$	500	2.15 (quasi-periodic)	$\lambda_4=-0.039\pm0.0001$ $\lambda_1=0.008\pm0.0002$	2.009 ± 0.03
$I=54.9$	500	2.6 (chaotic attractors)	$\lambda_2=-0.004\pm0.0002$ $\lambda_3=-0.026\pm0.0002$ $\lambda_4=0.040\pm0.0002$ $\lambda_1=0.015\pm0.001$ $\lambda_2=0.0021\pm0.002$ $\lambda_3=-0.032\pm0.001$ $\lambda_4=-0.062\pm0.001$	2.420 ± 0.04

not decay with the time. At $I=51.9$ mA, the ACF shows a quasi-periodic attractor, while for $I=54.9$ mA the ACF shows a chaotic attractor.

The LES was calculated at different discharge currents and sampling rates, 500 kHz, as represented in Fig. 5. At $I=48.2$ mA, the result attractor can be identified as $(0, -, -)$ within the error bars. The nonzero value of LES may be coming from the formation of the attractor, where the trajectories of the attractor diverge and converge in phase space. At $I=51.9$ mA the attractor is identified as $(0, 0, -)$, which indicates a quasi-periodic attractor, while at $I=54.9$ mA the attractor is identified as $(+, 0, -)$, which indicates a chaotic attractor.

The D_{corr} was calculated from the three time series at sampling rate 500 kHz as shown in Fig. 6. In m -dimensional embedding, we look for a plateau in the plot of $D_2(m, r)$ versus $\log(r)$, a range of r (the scaling region) over which $D_2(m, r)$ has a constant value or converges to a straight line. It is then taken to be the correlation dimension for the attractor. The length scale r is normalized to the largest distance in each embedding dimension. This is done in order to use a length scale derived from the size of the attractor. With this normalization, the correlation integral $C(m, r)$ reaches its maximum value (i.e., saturates) at the same value of r making it easier to compare the plateau for different embedding dimensions. For small values of r , as well as for large values of r , the correlation dimension increases with increasing the embedding dimension. The behavior at small values of r is characteristic of noise, which has infinite dimension. At large r 's, the increase of the slope is induced in part by using a relatively small number of embedding vectors in a high dimensional state. It becomes more pronounced and extends to smaller values of r as m is increased. Thus in the process of

increasing the embedding dimension, to check the convergence of the calculation, one uses the best value of D_{corr} , which is independent of m and r . At $I=48.2$ mA, the value of D_{corr} is an integer value, which indicates a periodic attractor. At $I=51.9$ mA, the value of D_{corr} denotes the quasi-periodic attractor. At $I=54.9$, the value of D_{corr} has a noninteger value that indicates a strange chaotic attractor with low dimension.

The results of numerical calculations are summarized in Table I.

- ¹B. Albrecht, H. Deutsch, R. W. Leven, and C. Wilke, Phys. Scr. **47**, 196 (1993); C. Wilke, H. Deutsch, and R. W. Leven, Contrib. Plasma Phys. **30**, 659 (1990).
- ²W. X. Ding, W. Huang, X. D. Wang, and C. X. Yu, Phys. Rev. Lett. **70**, 170 (1993); W. X. Ding, H. Deutsch, A. Dinklage, and C. Wilke, Phys. Rev. E **55**, 3769 (1997).
- ³T. Braun, J. A. Lisboa, R. E. Francke, and J. A. C. Gallas, Phys. Rev. Lett. **59**, 613 (1987).
- ⁴P. Y. Cheung and A. Y. Wong, Phys. Rev. Lett. **59**, 551 (1987).
- ⁵J. Qin, L. Wang, D. P. Yuan, P. Gao, and B. Z. Zhang, Phys. Rev. Lett. **63**, 163 (1989); D. L. Feng, J. Zheng, W. Huang, C. X. Yu, and W. X. Ding, Phys. Rev. E **54**, 2839 (1996).
- ⁶F. Greiner, T. Klinger, and A. Piel, Plasma Phys. **2**, 1810 (1995).
- ⁷T. Ueki, Y. Nishida, and N. Yugami, Phys. Rev. Lett. **76**, 4171 (1996).
- ⁸S. H. Fan, S. Z. Yang, J. H. Dai, S. B. Zheng, D. P. Yuan, and S. T. Tsai, Phys. Lett. A **164**, 295 (1992).
- ⁹R. Mane, D. Rand, and L. S. Young, *Warwick* (Springer, Berlin, 1981), p. 230.
- ¹⁰F. Takens, Detecting strange attractors in Turbulence, *Warwick* (Springer, Berlin, 1981), p. 366.
- ¹¹N. H. Packard, J. P. Gruchfield, J. D. Farmer, and R. S. Shaw, Phys. Rev. Lett. **45**, 712 (1993).
- ¹²P. Grassberger and I. Procaccia, Physica D **9**, 189 (1983).
- ¹³P. Grassberger and I. Procaccia, Phys. Rev. Lett. **50**, 346 (1983).
- ¹⁴A. Freund, Th.-Kruel, and F. W. Schneider in Proceedings from MIDIT 1986 Workshop, R. D. Parmentier and P. L. Christiansen, editors (Manchester University Press, 1987), p. 601.